PHYSICAL REVIEW E **69**, 065601(R) (2004)

Boosted propagation of femtosecond filaments in air by double-pulse combination

Luc Bergé
Département de Physique Théorique et Appliquée, Commissariat à l'Énergie Atomique, CEA/DAM-Ile de France, B.P. 12, 91680 Bruyères-le-Châtel, France

(Received 29 August 2003; revised manuscript received 11 February 2004; published 2 June 2004)

Two femtosecond pulses in convergent geometry are combined with an appropriate time delay, in order to double the length of the plasma channel created by multiphoton ionization of air. Suitable parameters are estimated analytically and tested by direct numerical simulations.

DOI: 10.1103/PhysRevE.69.065601 PACS number(s): 42.65.Tg, 42.65.Jx, 42.68.Ay

The propagation of femtosecond laser pulses in transparent media has become a topic of intense activities motivated by various applications, such as improving atmospheric remote sensing [1]. Among their numerous properties, ultrashort laser beams cover large propagation distances by forming self-guided filaments clamped at high intensities ($>10^{13}$ W/cm^2) with an electron plasma created by ionization of air molecules. This self-guiding of light results from the balance between the optical self-focusing (SF) of the beam and multiphoton ionization (MPI) of the medium. Along the propagation axis, MPI induces significant changes in the pulse temporal profile. Pulses with input power $P_{\rm in}$, far above the threshold power for SF, $P_{\rm cr}$, decay into multipeaked profiles, originating from the emergence of sharp ionization fronts. These fronts defocus the most intense time slices of the pulse, while letting others refocus at further longitudinal distances [2,5] and continue to feed the electron plasma.

Recently, the idea of combining several pulses for "boosting" the filamentation range was successfully tested in an experiment [6], where two twin pulses, launched collinearly in orthogonal polarization with an appropriate time delay, could double the total length of the plasma channel. This phenomenon, called "concatenation," was accompanied by a strong white-light emission and sub-terahertz radiation. Here, the technical choice of circularly polarized pulses was made to limit the interference fringes between the two pulses at zero delay. Several effects, as the energy exchanges between orthogonal modes, the strong shortening of one of the pulses, and their special time ordering, were proposed as key-players for this process [7]. However, orthogonal modes minimize energy exchanges [8], while pulse shortening cannot explain by itself how some temporal components in the earlier pulse catch the latest one at specific interpulse delays only. Thus, despite the preliminary works [6,7], a theory supporting the concatenation mechanism is still missing, which is the issue of the present investigation.

For clarity, we willingly forget the polarization geometry chosen in Ref. [6]. We consider linearly polarized pulses and remind of the standard propagation equations governing their envelope $\mathcal{E}(r,t,z)$ in air (see, e.g., Ref. [5])

$$\frac{\partial \mathcal{E}}{\partial z} = \frac{i}{2k_0}\vec{\nabla}_\perp^2 \mathcal{E} + ik_0 n_2 \left[\frac{|\mathcal{E}|^2}{2} + \frac{\tau^{-1}}{2}\int_{-\infty}^{t} e^{-(t-t')/\tau}|\mathcal{E}(t')|^2 dt' \right]\mathcal{E} - i\frac{k''}{2}\partial_t^2 \mathcal{E} - i\frac{k_0}{2\rho_c}\rho\mathcal{E} - \frac{1}{2}\sum_n \beta_n^{(K_n)}|\mathcal{E}|^{2K_n-2}\mathcal{E}, \quad (1)$$

$$\rho = \rho_{\rm at} - \rho_{\rm O} - \rho_{\rm N}, \quad \partial_t \rho_n = -\sigma_n |\mathcal{E}|^{2K_n}\rho_n, \quad (2)$$

where the index $n={\rm O,N}$ refers to oxygen or nitrogen species with ionization potentials $U_{\rm O}=12.1$ eV and $U_{\rm N}=15.6$ eV, respectively. Here, z is the propagation variable, $\vec{\nabla}_\perp^2 = r^{-1}\partial_r r\partial_r$ is the diffraction operator only depending on the radial variable r, t is the retarded time in the frame moving with the group velocity of light, $k_0=2\pi/\lambda_0$ for the wavelength $\lambda_0=800$ nm, $k''=0.2$ fs^2/cm is the coefficient of group-velocity dispersion, and n_2 is the nonlinear Kerr index entering the SF power $P_{\rm cr}=\lambda_0^2/2\pi n_2$. The Kerr response of air has a delayed component in ratio $1/2$ with characteristic time $\tau=70$ fs. In Eq. (2), the density of free electrons ρ is governed by MPI processes with coefficients $\sigma_{\rm O}=2.88\times10^{-99}$ s^{-1} cm^{16}/W^8 for oxygen ($K_{\rm O}=8$) and $\sigma_{\rm N}=5.08\times10^{-144}$ s^{-1} cm^{22}/W^{11} for nitrogen ($K_{\rm N}=11$). The constant $\beta_n^{(K_n)}=K_n\hbar\omega_0\sigma_n\rho_n$ is related to the nonlinear K_n-photon absorption from the different species n. The quantity $\rho_{\rm at}=2.5\times10^{19}$ cm^{-3} denotes the neutral density initially fixed with the proportions $\rho_{\rm O}(t\to-\infty)=0.2\rho_{\rm at}$ and $\rho_{\rm N}(t\to-\infty)=0.8\rho_{\rm at}$; $\rho_c=1.8\times10^{22}$ cm^{-3} is the critical plasma density. Constrained to the axial symmetry, Eq. (1) prohibits multiple filamentation. This approximation is however justified, since for the power levels examined here ($P_{\rm in}\sim10P_{\rm cr}$) femtosecond pulses should produce a single filament holding its spatial shape [3]. Also, electron recombination has been omitted in Eq. (2), as free electrons created in air have a lifetime larger than 10 ps [4], which widely exceeds the temporal delays below which two 100-fs pulses can interact.

Typically, plasma generation takes place over a distance $\Delta z_{\rm channel}\sim 2/\beta^{(K)}I_{\rm max}^{K-1}$, where $I_{\rm max}$ denotes the intensity of the self-guided filament realizing an equilibrium between SF and MPI. At IR wavelengths, multiphoton processes mainly ionize oxygen molecules and lead to $I_{\rm max}\sim5\times10^{13}$ W/cm^2,

while $\beta^{(K_O)} \sim 3\times 10^{-98}$ cm^{13}/W^7 [5]. The plasma channel is then expected to cover $\Delta z_{\text{channel}} = 0.85$ m, i.e., about 1 m for one pulse.

Let us now analyze two Gaussian pulses, being separated in time and focused by distinct converging lenses. Their temporal separation can be estimated, in such a way that, when the first pulse (pulse 1) ends to ionize air, the second one (pulse 2) begins to self-focus. Since SF preconditions plasma formation, we can first determine the collapse distances of two pulses with different lenses and given time delay. This is done by extending the "moving-focus model" [9] to a double-pulsed configuration. Although limited [10], this model offers a clear picture of the "temporal slices" in the incident beam that produce different collapse points, whose location over the z axis increases in inverse proportion to their power.

In the present context, the SF stage is governed by Eq. (1), in which we only retain the first four terms and freeze, for technical convenience, the temporal variations by fixing an effective instantaneous Kerr response with coefficient n_2^{eff}. This coefficient is approximated by searching for the time $t_{\max}$ at which the temporal dependencies in the total Kerr term of Eq. (1) are maximum. For Gaussian envelopes $\mathcal{E} \propto e^{-t^2/t_p^2}$ with temporal radius t_p, identifying $t_{\max}$ amounts to maximizing the function

$$F(t) = \frac{1}{2}e^{-2(t^2/t_p^2)} + \frac{\sqrt{\pi}t_p}{4\sqrt{2}\tau}e^{(t_p^2/8\tau^2)-(t/\tau)}\left[1 - \text{erf}\left\{\frac{t_p^2 - 4\pi t}{2\sqrt{2}\pi t_p}\right\}\right], \tag{3}$$

where erf(x) denotes the usual error function. Setting, e.g., $t_p = 102$ fs for pulses with 120-fs full width at half maximum diameter ($\equiv\sqrt{2\ln 2}\, t_p$), we find $t_{\max} = 13$ fs, so that $F(t_{\max}) \simeq 0.8$ yields $n_2^{\text{eff}} = 0.8\times n_2$. Thus, the action of the retarded Kerr component is to shift slightly the pulse to positive times and to increase its collapse distance to some extent.

In this approximation, we consider multipulsed beams governed by the reduced model $\partial_z\mathcal{E} = (i/2k_0)\vec{\nabla}_\perp^2\mathcal{E} + ik_0 n_2^{\text{eff}}|\mathcal{E}|^2$, with the effective critical power $P_{\text{cr}}^{\text{eff}} = \lambda_0^2/2\pi n_2^{\text{eff}}$. It is then well known that the mean-squared radius $\langle r^2\rangle = \int r^2|\mathcal{E}|^2 d\vec{r}/P$ of the beam satisfies [12]

$$Pd_z^2\langle r^2\rangle = 4H/k_0, \tag{4}$$

where $H = (1/2k_0)\|\vec{\nabla}_\perp\mathcal{E}\|_2^2 - (k_0 n_2^{\text{eff}}/2)\|\mathcal{E}\|_4^4$ is the Hamiltonian integral and $P \equiv \|\mathcal{E}\|_2^2$ is the beam power (by convention, $\|f\|_p^p \equiv \int |f|^p d\vec{r}$). Let us next introduce an input pulse defined at $z=0$ by the combination of two focused, collinear Gaussian subpulses

$$\mathcal{E}_{\text{in}}(r,t,0) = e^{-(r^2/w_0^2)}\sum_{i=1}^{2}\sqrt{\frac{2P_i}{\pi w_0^2}}e^{-ik_0 r^2/2f_i} \times h_i(t,\delta_i), \tag{5}$$

with identical waist w_0, individual power P_i, distinct focal lengths f_i, and temporal centroids δ_i entering the Gaussian components $h_i(t,\delta_i) \equiv e^{-(t-\delta_i)^2/t_p^2}$ ($i=1,2$). We assume symmetric centroids, $\delta_1 = -\delta_2 \equiv -\delta$, so that the temporal delay between the beam components is given by $\Delta = 2\delta$. Plugging Eq. (5) into H then yields

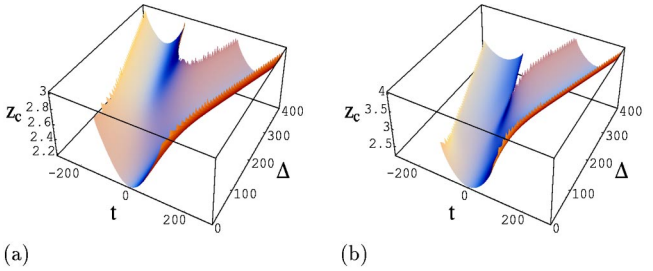

FIG. 1. z_c (m) vs time (fs) and Δ (fs) for (a) $f_1 = f_2 = 3$ m and (b) $f_1 = 3$ m, $f_2 = 4$ m, applied to 2.5 mJ pulses with $t_p = 102$ fs [$P_1 = P_2 = 5P_{\text{cr}}^{\text{eff}}$].

$$H = \frac{1}{2z_0}\left[\sum_{i=1}^{2}\left(1 + \frac{z_0^2}{f_i^2}\right)P_i h_i^2 - \frac{\mathcal{P}^2}{P_{\text{cr}}^{\text{eff}}} - 4\mathcal{P}'\left\{\frac{\mathcal{P}}{P_{\text{cr}}^{\text{eff}}(1+\kappa^2/16)} - \frac{\kappa^2 + (1-\kappa^2/4)(1+z_0^2/f_1f_2)}{2(1+\kappa^2/4)^2} + \frac{\mathcal{P}'(1+\kappa^2/8)}{P_{\text{cr}}^{\text{eff}}(1+\kappa^2/4)}\right\}\right], \tag{6}$$

where $\mathcal{P} \equiv \Sigma_{i=1}^2 P_i h_i^2$, $\mathcal{P}' \equiv \sqrt{P_1P_2}h_1h_2$, $\kappa \equiv z_0(f_1^{-1} - f_2^{-1})$, with $z_0 = k_0 w_0^2/2$. Integration of Eq. (4) provides the maximal collapse distances along the z axis

$$z_c(t,\Delta) = \frac{-d_z\langle r^2\rangle|_0 - \sqrt{d_z\langle r^2\rangle|_0^2 - 8H\langle r^2\rangle|_0/k_0P}}{4H/k_0P}, \tag{7}$$

$$Pd_z\langle r^2\rangle|_0 \equiv -w_0^2\left[\sum_{i=1}^{2}\frac{P_i h_i^2}{f_i} + \mathcal{P}'\frac{(1-\kappa^2/4)}{(1+\kappa^2/4)^2}(f_1^{-1} + f_2^{-1})\right], \quad P\langle r^2\rangle|_0 \equiv \frac{w_0^2}{2}\left[\sum_{i=1}^{2}h_i^2P_i + 2\mathcal{P}'\frac{(1-\kappa^2/4)}{(1+\kappa^2/4)^2}\right]. \tag{8}$$

Equation (7) supplies larger SF points than those evaluated by Marburger's empirical formula [9,11], when one analyzes the blow-up of one Gaussian component ($P_2 = 0$). In spite of this discrepancy, it can still yield reasonably good collapse ranges for the input powers ($P_{\text{in}}/P_{\text{cr}} \gg 1$) and lens curvatures selected here. Another limitation of this model is the absence of plasma generation. As is well known, MPI is expected to defocus the SF time slices with the highest power and let the others untouched [2]. By keeping this dynamics in mind, the present issue is not to describe the earliest defocusing events promoted by MPI, but rather to determine the appropriate range of time delays, inside which the *less powerful* time slices of pulse 1 can be connected with the most powerful ones in pulse 2, along the overall temporal input profile. This is actually the piece of information conveyed by Eq. (7), which may further be extended to more beams ($i \geqslant 2$) with different energies, shapes and focal lengths.

Figure 1 shows the surfaces formed by the collapse points

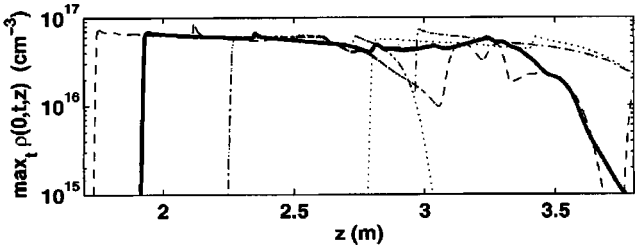

FIG. 2. Peak electron densities obtained from two 2.5 mJ pulses with duration $t_p=102$ fs and delays $\Delta=0$ fs (dashed curve), $\Delta=100$ fs (solid thick curve), and $\Delta=400$ fs (dash-dotted curve). The dotted lines, partly superimposed with the dash-dotted curve beginning from $z\simeq 2.25$ m, represent the electron plasma produced by the two pulses alone, separately focused with $f_1=3$ m and $f_2=4$ m.

z_c [Eq. (7)] versus time (t) and delay (Δ) for two pulses with $t_p=102$ fs, $w_0=3$ mm, and identical energies $E_{\rm in}=2.5$ mJ ($P_1=P_2=5P_{\rm cr}^{\rm eff}$), when choosing $f_1=3$ m. For $f_1=f_2$ [Fig. 1(a)], no enhancement of the SF distance occurs ($z_c\leqslant 3$ m), whatever the time delay between the two pulses may be. For $f_1=3$ m and $f_2=4$ m [Fig. 1(b)], the SF time slices of pulse 1, containing powers close to critical, match the earliest temporal slices that trigger SF in pulse 2, whenever the temporal delay lies nearby the pulse duration ($\Delta\simeq 100$ fs). The lens applied to the second pulse moves the focus along the z axis ($z_c\leqslant 4$ m), which results in enlarging the propagation range of the total pulse by about 1 m. This distance being of the order of $\Delta z_{\rm channel}$, the filaments generated by each pulse may then be locked *in one continuous channel* of around 2 m. This phenomenon cannot take place in the following two situations: Either $\Delta=0$, in which case SF mostly develops within a single sequence as two superimposed pulses behave as one high-power pulse, or $\Delta\gg t_p$, in which case the two pulses act as individual beams promoting separated filaments. This configuration is refound when the distance between the focal lengths is too large, e.g., $f_2>2f_1$. In that case, Eq. (7) predicts that the surfaces $z_c[t,\Delta]$ associated with the two collapsing pulses become disconnected.

To check our theoretical expectations, we have numerically integrated Eqs. (1) and (2) using the previous parameters ($f_1=3$ m, $f_2=4$ m). Figure 2 shows the peak electron densities arising from the minimum value $\rho_{\rm min}=10^{15}$ cm^{-3}. These are mainly fed by ionization of oxygen molecules. When $\Delta=0$, the electron density keeps a constant level over slightly more than 1 m, before decreasing suddenly at $z\simeq 3$ m. After this distance, residual bursts of free electrons end the self-guiding. For $\Delta=400$ fs, the plasma channel becomes discontinuous at the same distance of 3 m, which marks the frontier between the ionization domains of pulse 1 and pulse 2. When $\Delta=100$ fs, the excitation of free electrons appears to be quasicontinuous over almost 2 m. These results agree with the predictions inferred from Fig. 1.

Figure 3(a) illustrates the behaviors of the maximum-in-time intensity reached by the two-pulse combination over the same propagation interval. An important aspect is the "notch" formed around $z\simeq 2.95$ m-3 m, where the beam intensity significantly decreases up to $\delta I/I_{\rm max}\simeq 20\%\,(I\equiv|\mathcal{E}|^2)$ for the input delays $\Delta=0$ and $\Delta=400$ fs only. If we approxi-

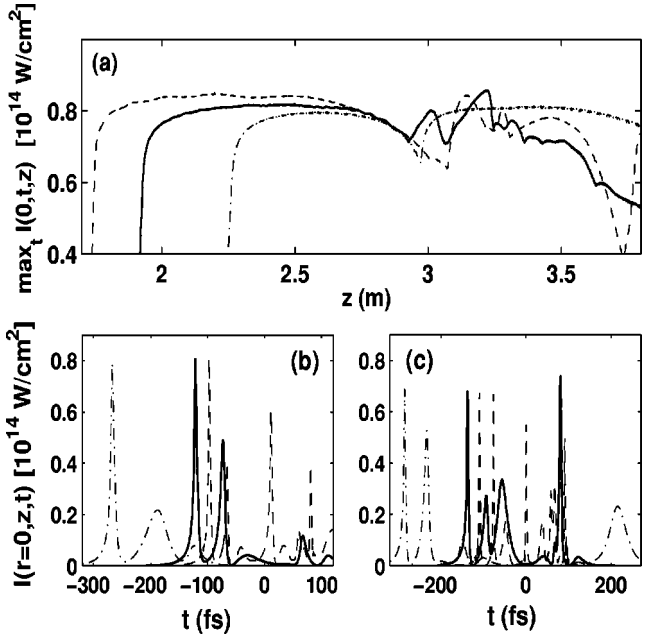

FIG. 3. (a) Peak intensity and (b), (c) temporal profiles produced by two-pulse combination in air at (b) $z=2.7$ m and (c) $z=3$ m for the delay $\Delta=0$ fs (dashed lines), and $z=2.95$ m for $\Delta=100$ fs (solid lines) and $\Delta=400$ fs (dash-dotted lines).

mate Eq. (2) as $\rho=t_p\sigma_{\rm O}I^{K_{\rm O}}\rho_{\rm O}$ by retaining the firstly ionized specy (oxygen) with exponent $K_{\rm O}=8$, the relative variations of ρ vs I express as $\delta\rho/\rho_{\rm max}=K_{\rm O}\delta I/I_{\rm max}$, where $\rho_{\rm max}\sim 2\rho_c n_2^{\rm eff}I_{\rm max}$ balances the Kerr effect. The notch in Fig. 3(a) is then sufficient to cause the discontinuity in the plasma range for $\Delta=0$ and 400 fs, starting from the numerical values $I_{\rm max}=8\times 10^{13}$ W/cm^2 and $\rho_{\rm max}=7\times 10^{16}$ cm^{-3}. In both cases, we indeed find $\delta\rho/\rho_{\rm max}>1.5$ and the electron density at the notch falls down by about one decade. In contrast, a delay of 100 fs preserves an intensity fluctuating below $\delta I/I_{\rm max}=6.25\%$, which guarantees an ionized channel undergoing fluctuations limited to $\rho_{\rm max}/2$.

Examining the temporal distortions in the pulse profile is also instructive. According to the "dynamic spatial replenishment" model [2], pulses with powers $\leqslant 10P_{\rm cr}$ first generate in the atmosphere a narrow leading peak resulting from the defocusing of their back part. Afterwards, they produce a trailing peak located in time at an interval close to $2t_p$ from their front edge. By choosing a temporal delay Δ in the vicinity of t_p, we thus select the optimal configuration for making the trail of pulse 1 coincide with the front edge of pulse 2 in ionization regime. Figures 3(b) and 3(c) show that for $\Delta=100$ fs the front peak of the first pulse ceases to keep up the electron plasma at $z=2.95$ m. Nevertheless, a trailing peak reinforced by the second pulse prolongates the plasma channel by reaching rapidly $I_{\rm max}$. Comparatively, a zero time delay involves the most powerful time slice available at center $[P_{\rm in}(t=0)=P_1+P_2+2\sqrt{P_1P_2}/(1+\kappa^2/4)\simeq 17P_{\rm cr}]$, which promotes the formation of many peaks during the first SF sequence [Fig. 3(b)]. These peaks dissipate most of the pulse energy and decrease too strongly before a second focusing cycle starts by linear lensing at $z=3$ m [Fig. 3(c)]. A long delay of 400 fs, instead, engages at $z=0$ a front pulse

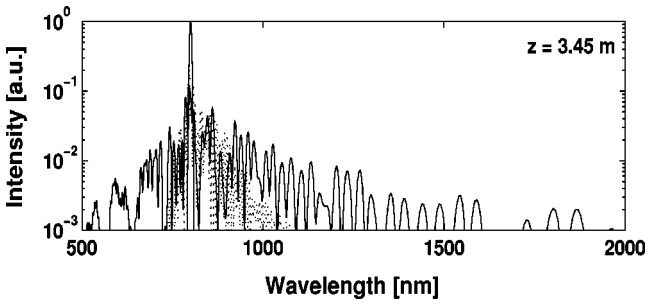

FIG. 4. Power spectra of two pulses in air, peaked at the input wavelength $\lambda_0 = 800$ nm and broadened for the time delays $\Delta = 100$ fs (solid curve) and $\Delta = 400$ fs (dotted curve). At $z = 3.45$ m, spectral broadening induced with $\Delta = 100$ fs was found to be nearly identical to that introduced with no delay.

with weaker power $[P_{\rm in}(t=-\Delta/2)=P_1+P_2e^{-2\Delta^2/t_p^2}+2\sqrt{P_1P_2}e^{-\Delta^2/t_p^2}/(1+\kappa^2/4)\approx P_1]$. However, the leading spike of pulse 1 diffracts too early at $z = 2.95$ m, for making the trail initiated by pulse 2 at $t = +200$ fs suitably connected to the first filament.

The above properties explain, with a good qualitative agreement, the experimental features revealed in Ref. [6]. Here, orthogonal 4-mJ pulses with waist $w_0 = 9$ mm conveyed each 10 critical powers, which justify quantitative differences in the SF distances and the effective power ratio $P_{\rm in}/P_{\rm cr}$. Also, the time ordering in delivering the two pulses was reverted ($\Delta \to -\Delta$). In this configuration, the leading edge of the latest pulse (1) connected with that of the earliest pulse (2) at an intensity level close to $I_{\max}$. Actually, our analysis shows that the attachment of fs filaments may be realized from a couple of pulses with different polarization geometry and time ordering.

Finally, we discuss the spectral broadening induced by the connection of two filaments. Figure 4 shows the power spectra occurring at $z = 3.45$ m with $\Delta = 400$ fs (dotted curve) and $\Delta = 100$ fs (solid curve). As it is clearly visible, the whole spectrum broadens four times more for the latter delay than for the former one, whose spectral enlargement covers that of a single pulse only [5]. This property can be understood from the elementary theory for self-phase modulation: Wavelength modulations are dictated by temporal variations as $\Delta\lambda/\lambda_0 = (1/\omega_0)\partial_t\phi$, where ϕ denotes the phase of $\mathcal{E}$. We may omit diffraction in SF regimes leading to an interplay with MPI ($\rho \sim |\mathcal{E}|^2$), in such a way that the phase ϕ still behaves like $\phi_z \sim k_0 n_2^{\rm eff}|\mathcal{E}|^2$. By using Eq. (5) in a first approximation, the spectral broadening reads as

$$\frac{\Delta\lambda}{\lambda_0} \approx -\frac{4k_0 n_2^{\rm eff}}{\omega_0 t_p^2}\Delta z \sum_{i=1}^{2} A_i h_i \times \sum_{i=1}^{2} A_i (t-\delta_i) h_i \qquad (9)$$

over an interval Δz, along which we suppose that the field with subpulse intensities A_i^2 does not vary in time. For two equal components ($A_1 = A_2$), the previous calculation emphasizes a symmetric spectral broadening with limited amplitude for well separated pulses ($\delta/t_p > 1$), whereas $\Delta\lambda/\lambda_0$ becomes at least doubled in both blue- and red-shift directions for overlapping Gaussian components ($\delta/t_p \leqslant 1$). This explains the wide broadening observed in the configuration $\delta \leqslant t_p$ (solid curve). A similar reasoning could be repeated for a more realistic situation involving subpulses being shorter in size, asymmetric, and separated by various delays: $\mathcal{E} = \Sigma_i A_i e^{-(t-\delta_i)^2/T^2}$ ($T \ll t_p$). Plotting $\Delta\lambda/\lambda_0$ would then display evidence of an enlarged spectrum whenever $\delta_i/T \approx 1$, which applies to peak distributions promoted by an initially small delay ($\Delta \leqslant 100$ fs), and of a narrower one for $\delta_i/T \gg 1$, which rather applies to pulse profiles favoring the noninteraction of their temporal components ($\Delta = 400$ fs).

In conclusion, we have developed a theoretical analysis of the concatenation mechanism discovered in Ref. [6], which allows us to noticeably enhance both the propagation range and power spectrum of femtosecond laser filaments in air with two focused pulses separated in time. The suitable temporal delay can be estimated from virial relations for wave collapse [Eq. (7)]. These provide the input key parameters allowing to lock together the ionized channels generated by each individual pulse, i.e., their time separation versus the difference in their focal lengths.

The author thanks Dr. H. Ward for preliminary numerical work on Eqs. (1) and (2).

[1] A. Braun *et al.*, Opt. Lett. **20**, 73 (1995); L. Wöste *et al.*, Laser Optoelektron. **29**, 51 (1997).
[2] M. Mlejnek, E. M. Wright, and J. V. Moloney, Opt. Lett. **23**, 382 (1998); L. Bergé and A. Couairon, Phys. Plasmas **7**, 210 (2000).
[3] S. L. Chin *et al.*, Appl. Phys. B: Lasers Opt. **74**, 67 (2002); F. Courvoisier *et al.*, Appl. Phys. Lett. **83**, 213 (2003).
[4] S. Tzortzakis, B. Prade, M. Franco, and A. Mysyrowicz, Opt. Commun. **181**, 123 (2000).
[5] A. Couairon *et al.*, J. Opt. Soc. Am. B **19**, 1117 (2002).
[6] S. Tzortzakis *et al.*, Appl. Phys. B: Lasers Opt. **76**, 609 (2003).
[7] A. Couairon *et al.*, Opt. Commun. **225**, 181 (2003).
[8] J. Schjödt-Eriksen *et al.*, Opt. Lett. **26**, 78 (2002).
[9] A. Brodeur *et al.*, Opt. Lett. **22**, 304 (1997).
[10] H. R. Lange *et al.*, Opt. Lett. **23**, 120 (1998).
[11] J. H. Marburger, Prog. Quantum Electron. **4**, 35 (1975).
[12] J. Juul Rasmussen and K. Rypdal, Phys. Scr. **33**, 481 (1986).